

## Microchannel evaporative CO<sub>2</sub> cooling for the LHCb VELO Upgrade

---

**Pablo Rodriguez Perez**<sup>\*†</sup>

*University of Manchester*

*E-mail:* [Pablo.Rodriguez@hep.manchester.ac.uk](mailto:Pablo.Rodriguez@hep.manchester.ac.uk)

The LHCb Vertex Detector (VELO) will be upgraded in 2018 to a lightweight pixel detector capable of 40 MHz readout and operation in very close proximity to the LHC beams. The thermal management of the system will be provided by evaporative CO<sub>2</sub> circulating in microchannels embedded within thin silicon plates. This solution has been selected due to the excellent thermal efficiency, the absence of thermal expansion mismatch with silicon ASIC's and sensors, the radiation hardness of CO<sub>2</sub>, and very low contribution to the material budget.

Although micro-channel cooling is gaining considerable attention for applications related to microelectronics, it is still a novel technology for particle physics experiments, in particular when combined with evaporative CO<sub>2</sub> cooling. The R&D effort for LHCb is focusing on the design and layout of the channels together with a fluidic connector and its attachment to withstand pressures in excess of 200 bars. This paper will describe the design and optimization of the cooling system for LHCb together with latest prototyping results.

Restriction channels are implemented before the entrance to a race-track layout of the main cooling channels. Restriction channels lengths were calculated to have the same total hydraulic resistance in all the channels. The coolant flow and pressure drop has been simulated as well as the thermal performance. These results can be compared to cooling performance measurements on prototype plates operating in vacuum. The design of a suitable low mass connector, together with the bonding technique to the cooling plate will be described.

Long term reliability as well as resistance to extremes of pressure and temperature is of prime importance. The setup and operation of a cyclic stress test of the prototype cooling channel designs will be described.

*Technology and Instrumentation in Particle Physics 2014,  
2-6 June, 2014  
Amsterdam, the Netherlands*

---

<sup>\*</sup>Speaker.

<sup>†</sup>On behalf of the LHCb VELO group.

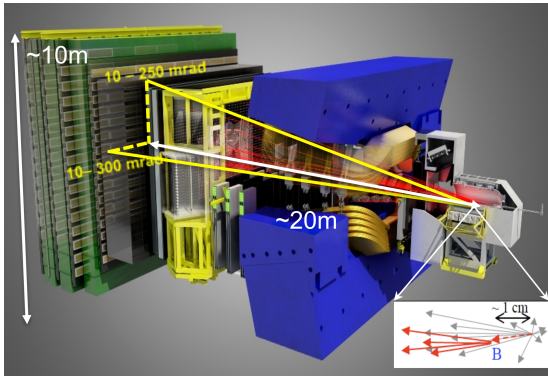


**Figure 1:** The LHCb experiment. An excellent vertex detector is necessary to identify the B mesons, which typically fly 1 cm before decay.

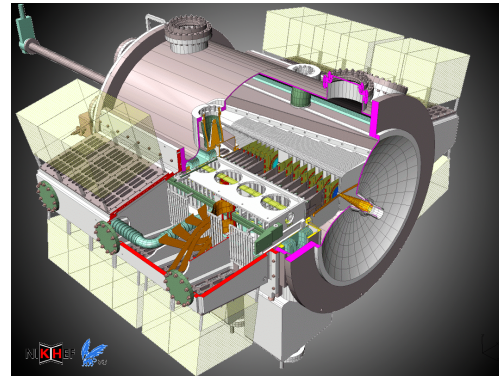


**Figure 2:** The VELO detector. Silicon sensors and front end electronics are placed in a secondary vacuum separated from the beam pipe by a thin foil.

## 1. The LHCb VERtEX LOcator

The LHCb experiment [1] searches for New Physics by studying CP Violation and rare decays of beauty and charm particles at the LHC. B mesons are typically produced at small angle with respect to the LHC beam, for that purpose the LHCb was build with a forward geometry (Fig. 1).

The VELO is the tracking detector surrounding the LHCb interaction region. Its responsibilities are to determine the interaction point and the secondary vertices belonging to particles which decayed shortly after the pp collision. To achieve the best resolution possible, the VELO modules are placed in a secondary vacuum (Fig. 2) as close to the beam as technically possible, starting the active area at 8.2 mm from the beam axis. The modules are separated from the primary vacuum by a corrugated 0.3 mm thick aluminium foil, which also shields the VELO electronics from the electronic pick-ups generated by the beam. For safety reasons, the modules are retracted to a safe position 3 cm away from the beam during injection, and moved back to nominal position once the beam is declared stable. Each of the 48 modules are made of 2 micro-strip sensors, providing the R and  $\phi$  coordinates of the hits. With this unique configuration the VELO can provide a single hit resolution down to 4  $\mu\text{m}$  and typical decay time resolution of 50 fs [2].

### 1.1 The VELO cooling

In the current VELO modules the sensors are attached to a carbon fibre structure which surrounds a Thermal Pyrolytic Graphite (TPG) central spine. The TPG has a high thermal conductivity ( $\sim 1500 \text{ W/mK}$ ) and takes the heat from the ASICs and sensors (total  $\sim 18 \text{ W}$ ) to the cooling blocks, placed at the base of the modules. In the cooling blocks the  $\text{CO}_2$  in liquid phase absorbs the heat from the TPG. This cooling system, which pioneered the use of two-phase  $\text{CO}_2$  cooling for particle physics, was developed by Nikhef in 2000.

$\text{CO}_2$  is an optimal choice as a 2-phase coolant for the VELO because it has high latent heat (2 KJ/kg·K) and low viscosity ( $1.45 \cdot 10^{-4} \text{ Pa} \cdot \text{s}$ ). These characteristics allow a cooling system to be built featuring small pipe diameters, allowing a reduction in the amount of material. In addition, the  $\text{CO}_2$  is radiation hard, cheap and environmental friendly.

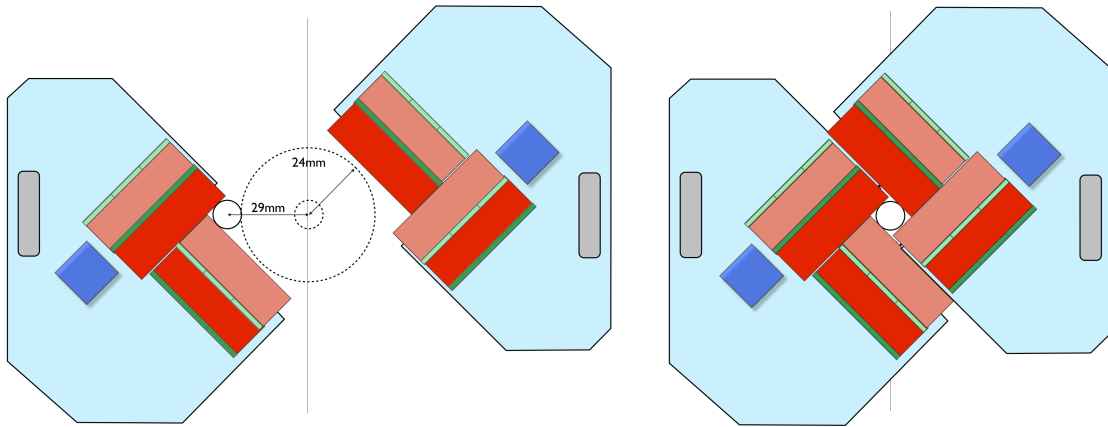


**Figure 3:** Front view of the VELO upgrade modules in the retracted position (left) and in closed position (right). Sensors glued on the back of the module are shown in pale red. Each sensor correspond to three ASICs, with readout pads overhanging under the sensors (in green). Light blue structures corresponds to the microchannel cooling plate, the grey rectangles are the connectors between the microchannels and the CO<sub>2</sub> pipes and the dark blue squares are the chips managing the slow and fast control signals.

The concept of the CO<sub>2</sub> cooling system of the current VELO performed so well [4] that it was decided to reuse the concept for the upgrade.

## 2. VELO Upgrade requirements

The LHCb experiment will be upgraded in 2018 to run at higher luminosities and being readout at 40 MHz instead of 1 MHz [5]. In addition the VELO sensors will be placed closer to the interaction point than the current detector, starting the active area at 5.1 mm. After an extensive review, it was decided to use pixels instead of micro-strips sensors for the VELO upgrade [6].

At the end of the sensors' lifetime, the irradiation in the inner regions of the sensors will be  $8 \times 10^{15}$  1MeVneq/cm<sup>2</sup> or 400 MRad for 50 fb<sup>-1</sup>. At this radiation dose the leakage current in a sensor will reach 200 μA/cm<sup>2</sup> at 1000 V and at -20°C at the position of the hottest pixel, generating up to 1 W of heat per sensor. To avoid thermal runaway an efficient cooling path is required.

The continuous readout at 40 MHz will generate 18 Gbit/s/ASIC for the hottest ASIC, which means 2.85 Tbit/s for the whole VELO. The ASICs closest to the interaction region will have the highest bandwidth requirements, generating up to 3 W of heat. The pixel ASIC is called VeloPix and it is being developed in collaboration between CERN and Nikhef. It has a matrix of 256 × 256 pixels, 55 × 55 μm each. The modules will have a L-shape, with two sensors at each side of the module, and three ASICs per sensor (Fig. 3).<sup>1</sup> In total, the cooling of the VELO upgrade must be capable of dealing with up to 36 W per module, while keeping a low material budget. An efficient and reliable cooling solution is a “must” for the pixel modules.

<sup>1</sup>A detailed explanation of the VELO upgrade is given in the talk “Upgrade of the Vertex Locator” by K. Akiba presented in this conference.

## 2.1 Cooling proposals for the VELO upgrade

**Cooling spine approach:** in the current VELO the cooling blocks are connected by a TPG spine to the heat sources, being separated by several centimetres. Simulations and thermal mock-up showed that under the conditions of the VELO upgrade the  $\Delta T$  across the module will be too high, leading to different expansions and risk of delamination.

**Cooling under the heat source approach:** an alternative approach was considered in which the coolant is circulated just below the heat sources. Two different proposals were studied:

- A carbon foam with a very high thermal conductivity is glued surrounding the titanium cooling pipes. On top of the carbon foam the ASICs and the hybrid with the slow control and readout chips are glued.
- Liquid CO<sub>2</sub> is circulated through microchannels etched inside a silicon plate, which also provides the mechanical support for the ASICs, sensors and hybrids.

It was demonstrated that both proposals satisfy the cooling requirements of the VELO upgrade. Nevertheless simulations of the impact parameter performance showed that the microchannels performed better than the carbon foam. This is a consequence of the extra material in the carbon foam proposal in the most critical areas of the acceptance, as it requires to place the titanium cooling pipes, which have significantly larger radiation length than silicon, just underneath the sensors. Additionally, as the microchannel plate is totally made on silicon, there is no CTE mismatch with the ASICs.

The complexity of the fabrication of microchannel plates and the attachment of the CO<sub>2</sub> cooling connector are the main drawback in comparison with the carbon foam approach. Luckily the fabrication process uses standard procedures already available in the industry so the production cost remains acceptable. The whole process needs more than 50 steps, including the DRIE etching of trenches using photolithography, the atomic bonding of the cover wafer to form capillaries and the thinning to 400  $\mu\text{m}$ . The final step in the factory is to DRIE etch the inlet and outlet holes.

## 2.2 The VELO upgrade module

The VELO upgrade modules will be L-shaped, with 2 sensors per side, and each sensor being bump-bonded to 3 VeloPix ASICs. The sensors closest to the interaction point will overhang by 5 mm over the microchannel plate (Fig. 4) in order to reduce the material budget between the interaction region and the first (and second) measured points. From simulations we know that we can expect a  $\Delta T = 8^\circ\text{C}$  between the tip of the sensor and the temperature of the microchannel at the maximum radiation dose. Therefore to keep the sensors below  $-20^\circ\text{C}$  the CO<sub>2</sub> coolant must be around  $-30^\circ\text{C}$ .

The pressure in the system will vary from 20 bar (at  $-30^\circ\text{C}$  which is the operational temperature) up to 60 bar (at  $+25^\circ\text{C}$  which is installation and maintenance temperature). The microchannel plates are designed to reliably hold 150 bars, which means a safety margin of 2.5.



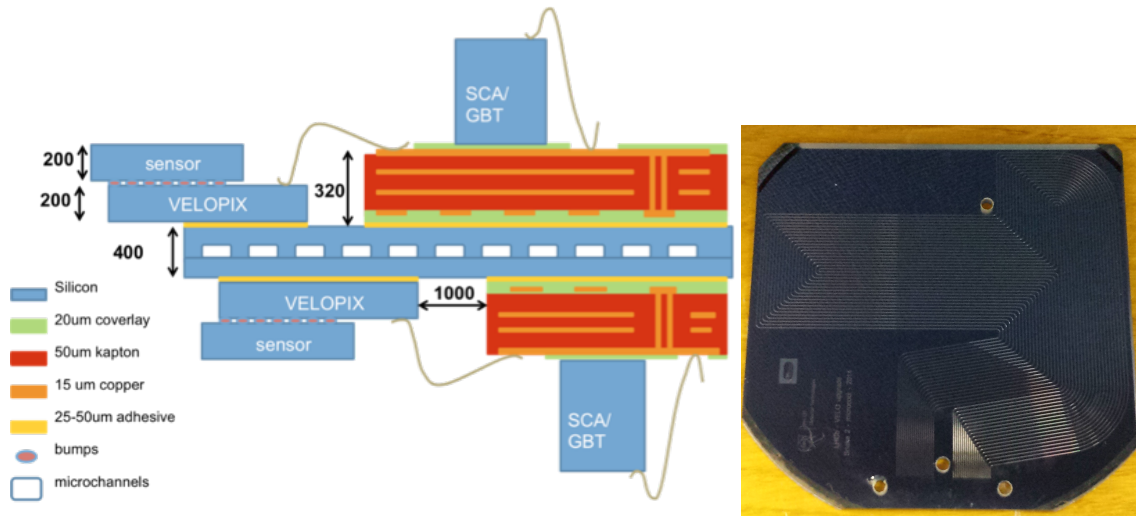


**Figure 4:** On the left, cross section of the VELO upgrade module. On the right, photo of the current microchannel plate which is being tested.

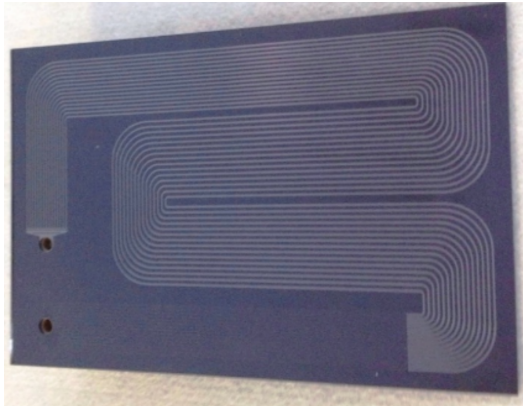


**Figure 5:** Photograph of the first microchannel prototype bonded to a 5 mm Pyrex sheet.

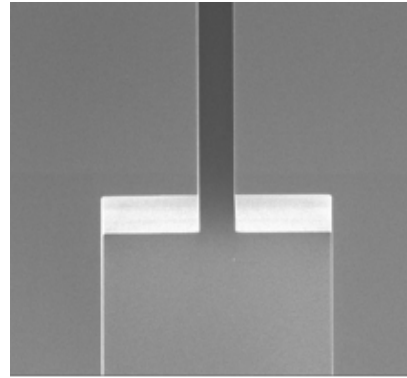


**Figure 6:** Photograph of the transition between restriction channels (top) and evaporation channels (bottom).

### 3. Microchannel studies

#### 3.1 First prototype

A *proof of principle* microchannel prototype was produced and CO<sub>2</sub> in a 2-phase stable condition was successfully circulated through it during 2012 [7]. The prototype was made by bonding a 760 μm silicon wafer with the etched channels to a 5 mm Pyrex plate (Fig. 5). The liquid CO<sub>2</sub> enters in the microchannel plate by a circular inlet hole (500 μm diameter). The narrow channels connected to the inlet are the so-called restriction channels. These channels are 30 μm wide and represent the main impedance in the cooling circuit, where the pressure drops until the liquid CO<sub>2</sub> reaches the boiling point. The change of phase is triggered in the transition point where the channel dimensions increases to 200 μm. Along the main channels the CO<sub>2</sub> evaporates under nearly isothermal conditions.

More microchannel samples with different layouts were produced after this first prototype. Extensive tests probed the capability of the silicon to hold pressures well beyond the safety margin imposed. The layout was modified to a more realistic pattern with the L-shape of the VELO upgrade module. The length of the restriction channels was re-calculated to balance the different length of the evaporation channels and present the same overall flow resistance. The connectors were also redesigned to improve the safety. All these changes are detailed in the next sections.

### 3.2 Wafer bonding

The bonding of the silicon wafers is the most critical steps in the microchannel fabrication. Two different techniques to perform the atomic bonding were tested:

- **Hydrophilic bonding:** the silicon wafers are covered by water and the silicon atoms of the surface join to oxygen atoms. During the atomic bonding of the wafers, the silicon oxide layer becomes the bonding interface.
- **Hydrophobic bonding:** the atomic bonding is directly Si-Si. It is a more complicated bonding process and the surfaces must be completely clean and free of imperfections.

Several hundred of samples were manufactured by *LETI* [10], and the quality of the bonding was monitored with surface acoustic microscopy. These samples underwent high pressure tests, showing that the hydrophilic samples can hold up to 400 bar, while the hydrophobic could hold probably more than 700 bars, which was the pump limit, without rupture. The analysis of the hydrophilic samples showed that occasionally in some areas the wafers were not bonded. Both bonding processes satisfy by far the 150 bar minimum pressure tolerance. No decision has yet been taken for the production.

### 3.3 Wafer thickness

The pressure that the silicon wafer can hold was studied as function of the thickness. Several samples were produced with 3 different microchannels width, 100, 200 and 500  $\mu\text{m}$ . These silicon samples were bonded to 2 mm of glass, and the rupture values are shown in Fig. 7. The test shows that with a channel width of 200  $\mu\text{m}$ , a thickness of 40  $\mu\text{m}$  was enough to hold 350 bar of pressure. A value of 140  $\mu\text{m}$  thick silicon was chosen due to mechanical reasons, as the microchannel plate is the structure which will hold the sensors and the hybrid. Therefore, the microchannel plate will have no problem to safely hold  $\text{CO}_2$  at 150 bars.

### 3.4 Endurance test

The hydrophilic and hydrophobic samples were tested after temperature and pressure cycles. The pressure was provided by pressurized air, and the temperature cycles by a Peltier plate. The pressure range was from 1 up to 200 bars, and the temperature varied between  $-40^\circ\text{C}$  to  $+40^\circ\text{C}$ , with 14 pressure cycles per temperature cycle. After more than 1000 cycles, none of the samples showed rupture.

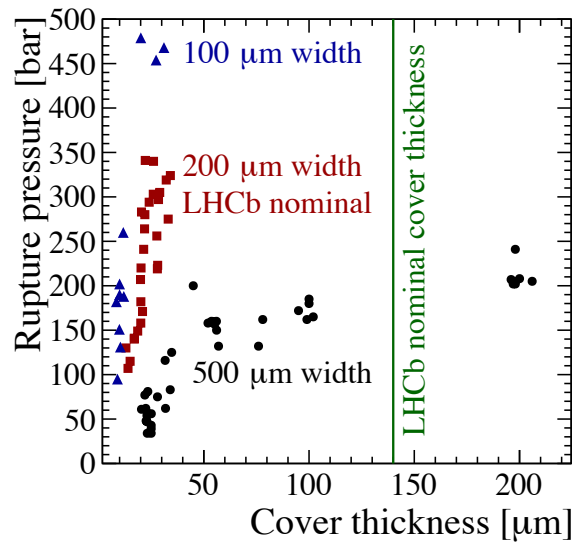


**Figure 7:** Maximum pressure that a 100, 200 and 500  $\mu\text{m}$  wide silicon channel can hold as function of the silicon thickness. The nominal cover thickness is the minimum required for mechanical reasons.

### 3.5 Layout enhancement

#### 3.5.1 Channel spacing

In the first prototype the distance between the microchannels were arbitrary chosen to be equal to the channel width, 200  $\mu\text{m}$ . Simulations with ANSYS [9] showed that with such granularity the heat is absorbed only by the upper and lower microchannel surfaces, so new simulations were carried out to determine the optimal spacing values. The goal was to use effectively the side walls of the microchannel to absorb heat. The counter-effect of a higher spacing is an increase of the  $\Delta T$  on the silicon surface ( $< 1\text{ }^\circ\text{C}$ ). As compromise solution a spacing of 500  $\mu\text{m}$  between the channel walls was chosen, which implies a  $\Delta T = 0.5^\circ\text{C}$  in the silicon surface.

#### 3.5.2 Channel dimensions

The pressure resistance test showed that a cover thickness of 140  $\mu\text{m}$  is sufficient to hold the pressures. With a total substrate thickness of 400  $\mu\text{m}$  the channel height can therefore be increased to 120  $\mu\text{m}$  in the main channels. The main channel width was kept unchanged to 200  $\mu\text{m}$ .

The restriction channels cross section were changed from rectangular ( $30 \times 70\text{ }\mu\text{m}$ ) to square ( $60 \times 60\text{ }\mu\text{m}$ ), making them less susceptible to obstruction by micro-particles. These modifications have lowered the flow resistance, for laminar single-phase flow, by a factor of 4 compared to the original layout, while keeping the ratio of the hydraulic resistance of the restriction channels to the main channels constant around 10. These calculations were based on the formulas from [8]. The high flow resistance of the restriction channels guarantees equal flow distribution among the many parallel channels.

### 3.6 Fluidic connector

The fluidic connector is the interface between the cooling pipes and the microchannel plate. During the pressure test it was proven to be one of the most critical components of the cooling

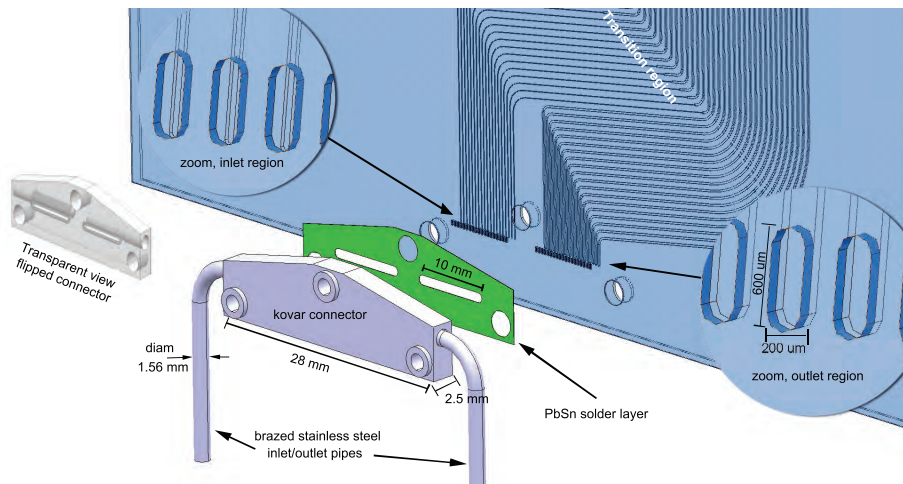


**Figure 8:** Fluidic connector between the cooling pipe and the microchannel plate.

system. In order to reduce the risk of rupture, and enhance the liquid flow, the inlet and outlet holes were re-designed.

In the new design (Fig. 8) the inlet holes in the Si are now  $200\ \mu\text{m}$  by  $600\ \mu\text{m}$  instead of circular holes of  $500\ \mu\text{m}$ .

With these dimensions the overall surface increases by a factor of 10, easing the connection between the channels and the pipes. Furthermore, the new design is safer than the old one because now the critical dimension is  $200\ \mu\text{m}$  instead of  $500\ \mu\text{m}$ .

The technique to attach the connector to the silicon plate was studied. Eutectic soldering with a layer of Pb-Sn between the connector and the plate was tested, reaching an attachment force above  $580\ \text{N}$  in the pull test and holding  $400\ \text{bar}$  without rupture.

Currently the effort is focused on creep effect over time studies and resistance to thermal cyclic tests.

## 4. Thermal performance

### 4.1 Thermal simulation

The temperature in the sensors surfaces was simulated with ANSYS (Fig. 9). The simulation conditions were an extreme case scenario, assuming a heat source of  $3\ \text{W}$  per ASIC. The thermal interface between the ASICs and the microchannel plate in the simulation was a  $100\ \mu\text{m}$  thick layer of Stycast 8550FT with Catalyst 9. In the simulation the temperature of the liquid  $\text{CO}_2$  in the inlet was  $-30^\circ\text{C}$ . The result of the simulation was a  $\Delta T = 7.4^\circ\text{C}$  between the overhanging sensor tip and the microchannel plate.

### 4.2 Thermal mock-up

Two pieces of metalized silicon were built to replicate the expected heat distribution generated by two irradiated sensors with 3 ASICs each. These heaters were glued to the proof-of-principle microchannel plate, one of them overhanging  $5\ \text{mm}$  as in the L-shape module. Three temperature

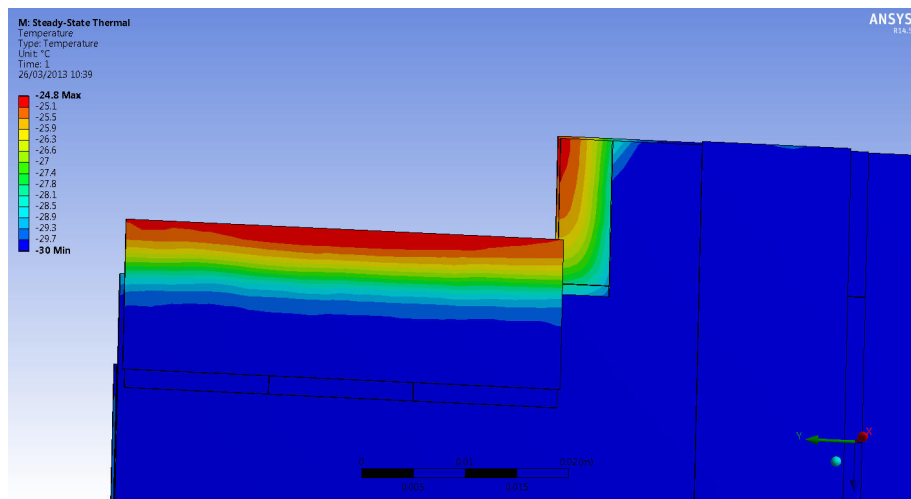


**Figure 9:** Thermal simulation of the temperature in the overhanging sensor in extreme case scenario: 3 W/ASIC, 100  $\mu\text{m}$  thick glue and  $\text{CO}_2$  circulating at  $-30^\circ\text{C}$ .

sensors were glued to the heaters to measure the temperature in the overhanging sensor tip, and two other locations where a  $\Delta T$  was expected.

The measurements showed a constant  $\Delta T = 3^\circ\text{C}$  between the first two channels, while the  $\Delta T$  between the sensor tip and the coolant increases with the dissipated power, but remaining below  $8^\circ\text{C}$ .

## 5. Conclusions

Evaporative  $\text{CO}_2$  cooling using microchannels in a  $400\ \mu\text{m}$  thick silicon device satisfies our cooling requirements in terms of material budget, power density and maximum temperature in the overhanging sensor tip. The reliability of the microchannel under high pressure conditions and temperature/pressure cycling test was demonstrated. The layout of the microchannels was optimized to enhance the cooling power and reduce the hydraulic resistance of the cooling circuit. The connector strength and leak tightness was demonstrated, and current effort is focused on connector reliability test.

## References

- [1] A. A. Alves Jr et al., *The LHCb detector at the LHC*, JINST 3, S08005, 2008 (DOI:10.1088/1748-0221/3/08/S08005).
- [2] R. Aaij et al., *Performance of the LHCb Vertex Locator*, accepted by JINST, arXiv:1405.7808 [physics.ins-det], 2014.
- [3] B. Verlaet et al., *CO<sub>2</sub> Cooling for the LHCb-VELO Experiment at CERN*, 8th IIF/IIR Gustav Lorentzen Conference on Natural Working Fluids, Copenhagen Denmark, 2008.
- [4] Eddy Jans, *Operational aspects of the VELO cooling system of LHCb*, Vertex2013, p038, PoS, 2013.
- [5] R. Aaij et al., *Framework TDR for the LHCb Upgrade*, CERN-LHCC-2012-007. LHCb-TDR-012, 2012.

- [6] LHCb Collaboration, *LHCb VELO Upgrade Technical Design Report*, CERN-LHCC-2013-021. LHCb-TDR-013, 2013.
- [7] A. Nomerotski et al., *Evaporative CO<sub>2</sub> cooling using microchannels etched in silicon for the future LHCb vertex detector*, JINST 8 P04004, 2013 (DOI:10.1088/1748-0221/8/04/P04004).
- [8] M. Fuerstman, A. Lai, A. Meghan, E. Thurlow, S. Shevkoplyas, H. Stone and G. Whitesides, *The pressure drop along rectangular microchannels containing bubbles*, Advanced Article on the web 22nd August 2007 (DOI: 10.1039/b706549c)
- [9] ANSYS® Academic Research, Release 14.5, ANSYS, Inc.
- [10] LETI Micro and nanotechnologies. Commissariat à l'Énergie Atomique, 85 X, 38041 Grenoble Cedex, France.